JOURNAL OF BACTERIOLOGY, Apr. 2005, p. 2628–2637 Vol. 187, No. 8
0021-9193/05/$08.00+0 doi:10.1128/JB.187.8.2628–2637.2005

Flavobacterium johnsoniae GldJ Is a Lipoprotein That Is Required for Gliding Motility

Timothy F. Braun and Mark J. McBride*

Department of Biological Sciences, University of Wisconsin—Milwaukee, Milwaukee, Wisconsin

Received 13 December 2004/Accepted 10 January 2005

Cells of *Flavobacterium johnsoniae* glide rapidly over surfaces by an unknown mechanism. Eight genes required for gliding motility have been described. Complementation of the nonmotile mutant UW102-48 identified another gene, *gldJ*, that is required for gliding. *gldJ* mutants formed nonspreading colonies, and individual cells were completely nonmotile. Like previously described nonmotile mutants, *gldJ* mutants were deficient in chitin utilization and were resistant to bacteriophages that infect wild-type cells. Cell fractionation and labeling studies with [^{3}H]palmitate indicated that GldJ is a lipoprotein. Mutations in *gldA*, *gldB*, *gldD*, *gldF*, *gldG*, *gldH*, or *gldI* resulted in normal levels of *gldJ* transcript but decreased levels of GldJ protein. Expression of truncated GldJ protein in wild-type cells resulted in a severe motility defect. GldJ was found in regular bands that suggest the presence of a helical structure within the cell envelope.

Cells of the bacterium *Flavobacterium johnsoniae* move rapidly over surfaces in a process called gliding motility. Rapid gliding motility is common in the large and diverse phylum of bacteria known as the bacteroidetes, of which *F. johnsoniae* is a member. Cells of *F. johnsoniae* move at speeds of up to 10 μm/s. They also absorb latex spheres and propel these rapidly around the cell in multiple paths. Several models have been proposed to explain this type of gliding motility, but the structures that comprise the motility machinery and the mechanism of cell movement remain unknown (28).

Gliding motility is not confined to the bacteroidetes but is also found in members of many branches of the bacterial phylogenetic tree (28). Recent results suggest that there are several different types of gliding "motors" that probably evolved independently. Extension and retraction of type IV pili are responsible for gliding of *Synechocystis* strain PCC6803, "social gliding motility" of *Myxococcus xanthus*, and twitching motility of *Pseudomonas aeruginosa* and other bacteria (5, 23, 27, 48). In contrast, *M. xanthus* "adventurous gliding motility" and gliding of filamentous cyanobacteria may be powered by polysaccharide secretion (18, 49), while mycoplasma gliding is thought to involve the cytoskeleton (25, 35). The motor responsible for bacteroidete gliding is not yet known, but genetic and behavioral studies of *F. johnsoniae* suggest that it may be unrelated to those described above (29).

Genetic techniques have been developed for *F. johnsoniae*, and genes that are required for motility have been identified (32). *gldA*, *gldF*, and *gldG* encode proteins that are thought to form an ATP-binding cassette transporter that is required for gliding (1, 19). Four lipoproteins that are required for movement (GldB, GldD, GldH, and GldI) have also been identified (20, 21, 30, 31). Mutations in any of these genes result in loss of gliding motility, inability to propel latex spheres along the cell surface, deficiency in the ability to digest the insoluble polysaccharide chitin, and resistance to bacteriophages that infect wild-type cells. The connection among gliding motility, chitin utilization, and infection by bacteriophages is not known, but it has been suggested that one or more transporters may be required for each of these processes (31). This paper describes the identification of *gldJ*, which encodes another lipoprotein that is required for gliding. Immunolocalization of GldJ reveals a first glimpse of the motility machinery and suggests that it may have a helical component in the cell envelope.

MATERIALS AND METHODS

Bacterial and bacteriophage strains, plasmids, and growth conditions. *F. johnsoniae* UW101 (from the *F. johnsoniae* type strain ATCC 17061) was the wild type used in this study, and all mutants were derived from this strain (30). The 50 spontaneous and chemically induced nonmotile mutants of *F. johnsoniae* (obtained from J. Pate) were previously described (7, 21, 51). The bacteriophages active against *F. johnsoniae* that were used in this study were ϕCj1, ϕCj7, ϕCj13, ϕCj23, ϕCj29, ϕCj42, ϕCj48, and ϕCj54 (7, 37, 51). The *Escherichia coli* strains used were DH5αMCR (Gibco BRL Life Technologies), S17-1 (46), and TOP10 (Invitrogen). *E. coli* strains were grown in Luria-Bertani medium at 37°C, and *F. johnsoniae* strains were grown in Casitone yeast extract (CYE) medium at 30°C, as previously described (32). To observe colony spreading, *F. johnsoniae* was grown on PY2 agar medium (1) at 25°C. Chitin utilization was observed as previously described (30). Antibiotics were used at the indicated concentrations when needed: ampicillin, 100 μg/ml; erythromycin, 100 μg/ml; kanamycin, 30 μg/ml; and tetracycline, 20 μg/ml. Plasmids and primers used in this study are listed in Table 1.

Cloning of *gldJ*. GldJ was cloned from a cosmid library of wild-type *F. johnsoniae* DNA in pCP26 essentially as previously described (21). Cosmids were transferred into the nonmotile mutant UW102-48 by conjugation, and complemented (spreading) colonies were isolated. Cosmids were isolated from spreading colonies, and subclones were generated from one of these (pCP432) to determine the minimal region required for complementation (Fig. 1). pMM265 was constructed by inserting the 3.1-kbp PstI fragment of pCP432 which spans *gldJ* into pCP11. A 1.9-kb fragment spanning just *gldJ* was amplified using Expand polymerase and primers 655 and 656 and inserted in both orientations into the SmaI site of pCP11 to generate pMM313 and pMM314. A modified version of *gldJ* encoding eight histidine residues at the carboxy terminus was constructed by amplification with Elongase (Gibco Life Technologies) and primers 227 and 573. The product was ligated into the SmaI site of pCP23 to generate pTB44, which encodes functional GldJ-His. Plasmids pMM315, pMM316, pMM317, and pMM318, which encode truncated forms of GldJ, were constructed by modifying pMM313. pMM313 was cut with EcoRV and NotI, treated with DNA polymerase Klenow fragment, and ligated to form pMM315, which encodes the first 337 amino acids of GldJ followed by 57 additional vector-encoded amino acids at the

* Corresponding author. Mailing address: Department of Biological Sciences, 181 Lapham Hall, University of Wisconsin—Milwaukee, 3209 N. Maryland Ave., Milwaukee, WI 53211. Phone: (414) 229-5844. Fax: (414) 229-3926. E-mail: mcbride@uwm.edu.

TABLE 1. Plasmids and primers used in this study[a]

Plasmid or primer	Description and/or sequence	Reference or source
Plasmids	Description	
pT7Blue	ColE1 *ori*; Ap^r	Novagen
pBAD/His-B	ColE1 *ori*, His tag expression vector; Ap^r	Invitrogen
pSTBlue-1	ColE1 *ori*; Ap^r	Novagen
pSBET	pACYC177-based plasmid carrying the rare $tRNA_{Arg}$-encoding gene *argU*; Cm^r	44
pCP11	*E. coli-F. johnsoniae* shuttle plasmid; Ap^r (Em^r)	32
pCP23	*E. coli-F. johnsoniae* shuttle plasmid; Ap^r (Tc^r)	1
pCP26	*E. coli-F. johnsoniae* shuttle cosmid; Km^r Tc^r (Em^r)	21
pCP432	Cosmid clone carrying *gldJ*; Km^r Tc^r (Em^r)	This study
pJW201	1.65-kbp PCR product containing 3′ end of *gldJ* cloned into pSTBlue-1; Ap^r	This study
pMM265	3.1-kbp PstI fragment of pCP432 (spanning *gldJ*) in pCP11; Ap^r (Em^r)	This study
pMM313	1.9-kbp PCR product spanning *gldJ* cloned into the SmaI site of pCP11; Ap^r (Em^r)	This study
pMM314	1.9-kbp PCR product spanning *gldJ* cloned into the SmaI site of pCP11 (opposite orientation of pMM313); Ap^r (Em^r)	This study
pMM315	Fragment encoding the first 337 amino acids of GldJ inserted in pCP11; Ap^r (Em^r)	This study
pMM316	Fragment encoding the first 548 amino acids of GldJ inserted in pCP11; Ap^r (Em^r)	This study
pMM317	Fragment encoding the first 337 amino acids of GldJ inserted in pCP11; Ap^r (Em^r)	This study
pMM318	Fragment encoding the first 547 amino acids of GldJ inserted in pCP11; Ap^r (Em^r)	This study
pTB37	*gldJ* expression plasmid, 1.65-kbp EcoRI-BglII fragment of pJW201 in pBAD/His-B; Ap^r	This study
pTB44	Recombinant *gldJ-his* in pCP23; expresses GldJ with a carboxy-terminal His tag; Ap^r (Tc^r)	This study
pTB45	Recombinant *gldI-his* in pCP23; expresses GldI with a carboxy-terminal His tag; Ap^r (Tc^r)	30
Primers		
227	5′ GAATTTGAAATCGCAGCCG 3′; primer used for construction of pTB44	
232	5′ CATATTGGTTACCTCTGTAGTAGTTG 3′ used for RNA analysis	
478	5′ CATCTACAACTTATGGTGGAAATG 3′ used for RNA analysis	
510	5′ ACGGCTAGATCTAGCAAAAAATCGAGTTCG 3′; primer used for construction of pJW201 and pTB37 (*gldJ*-His)	
511	5′ TTTTATGAATTCTTCTTTATCTTAATTTCTTGGTG 3′; primer used for construction of pJW201	
573	5′ TTATTAATGATGATGATGATGATGATGATTTCTTGGTGATTTTCTTCTTTCAG 3′; primer used during construction of pTB44	
655	5′ TTGTATCAATTGAAAGAGATTGG 3′; primer used for construction of pMM313 and pMM314	
656	5′ TAGTATAAAGTATGCGATCAGGG 3′; primer used for construction of pMM313 and pMM314	

[a] Antibiotic resistance phenotypes: ampicillin, Ap^r; erythromycin, Em^r; kanamycin, Km^r; tetracycline, Tc^r. Unless indicated otherwise, antibiotic resistance phenotypes are those expressed in *E. coli.* Antibiotic resistance phenotypes listed in parentheses are those expressed in *F. johnsoniae* but not in *E. coli.*

carboxy terminus. pMM313 was cut with XbaI, and the 11.2-kb fragment was circularized and ligated to form pMM316, which encodes the first 548 amino acids of GldJ followed by 53 vector-encoded amino acids. pMM315 and pMM316 were modified to generate pMM317 and pMM318, respectively, which produced truncated GldJ proteins without the long C-terminal vector-encoded tails. This was done by digesting the plasmids with XbaI, filling in the ends with DNA Klenow polymerase, and joining the ends by ligation. pMM317 encodes the first 337 amino acids of GldJ followed by four amino acids (GRSS). pMM318 encodes

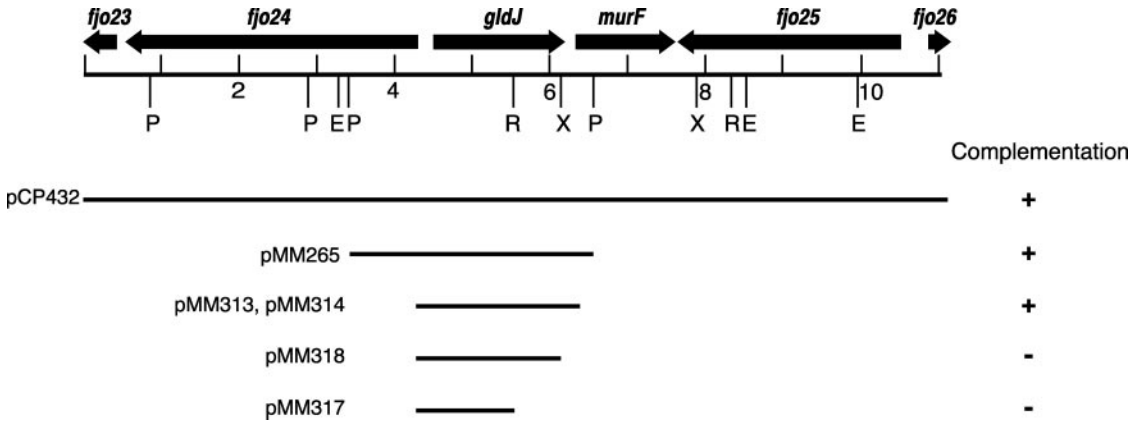

FIG. 1. Map of the *gldJ* region of *F. johnsoniae*. Restriction sites are indicated as follows: E, EcoRI; P, PstI; R, EcoRV; X, XbaI. Numbers below the map refer to kilobase pairs of sequence. The presence (+) or absence (−) of complementation of *gldJ* mutants by fragments cloned into shuttle vectors is indicated beneath the map.

the first 547 amino acids of GldJ followed by a serine. For complementation analyses, plasmids were introduced into the *F. johnsoniae* mutants by conjugation or electroporation as previously described (21, 32).

Nucleic acid sequencing. Nucleic acid sequencing was performed by the dideoxy nucleotide procedure with an automated (Applied Biosystems) sequencing system. Sequences were analyzed with the MacVector and AssemblyLign software (Oxford Molecular Group Inc., Campbell, Calif.), and comparisons to database sequences were made using the BLAST (2) and FASTA (38) algorithms. Predictions regarding cellular localization were made using PSORT (http://psort.nibb.ac.jp/) (36).

RNA analysis. Total RNA was isolated from overnight cultures of *F. johnsoniae* by using RNeasy and RNA Protect bacterial reagent (Qiagen) or by cold phenol extraction (43). Northern blotting was performed essentially as described previously (42). Probes were made using the DIG RNA labeling kit (Roche Diagnostics Corp.). An internal fragment of *gldJ* was amplified using primers 232 and 478. Products were purified by agarose gel electrophoresis and ligated into pT7Blue. The ligation products were used as template in a second amplification with the T7 primer and primer 478. The product was used for in vitro transcription to produce the digoxigenin-labeled probe.

Protein expression and antibody production. A 1,647-bp fragment encoding the C-terminal 541 amino acids of GldJ was amplified using Elongase and primers 510 and 511 and cloned into the EcoRV site of pSTBlue-1 to generate pJW201. The EcoRI-BglII fragment of pJW201 containing *gldJ* was ligated into pBAD-HisB to produce pTB37. pSBET (44), which encodes a rare Arg tRNA required for efficient expression of *gldJ* in *E. coli*, was introduced into *E. coli* TOP10 cells carrying pTB37. To isolate recombinant GldJ, cells were grown to mid-log phase at 37°C in Luria broth, induced by the addition of 0.05% arabinose, and incubated for an additional 2 h. Cells were disrupted using a French press, and inclusions containing recombinant GldJ were isolated by centrifugation at 6,000 × *g* for 10 min and washed twice in a buffer consisting of 50 mM Tris (pH 7.9), 500 mM NaCl, and 1% Triton X-100. The GldJ inclusions were solubilized in 5 M urea plus binding buffer (50 mM Tris [pH 7.9], 500 mM NaCl, 0.05% Triton X-100, and 5 mM imidazole) at 50°C. Insoluble material was pelleted by centrifugation (10,000 × *g* for 15 min), and the supernatant was applied to ProBond Ni affinity resin (Invitrogen). GldJ-His bound tenaciously to the resin and was not eluted by repeated washings with binding buffer containing 300 mM imidazole and with binding buffer containing 30 mM EDTA. GldJ was recovered by stripping nickel from the resin with 30 mM EDTA and then denaturing GldJ-His with binding buffer plus 5 M urea at 50°C to release the protein. Urea was removed by dialysis, and GldJ-His was equilibrated in 50 mM sodium phosphate (pH 7.4)–150 mM NaCl–0.05% Triton X-100.

Polyclonal antibodies were produced in New Zealand White rabbits by Covance (Denver, Pa.). Samples of the polyclonal antisera and preimmune sera were affinity purified using GldJ-His immobilized on Pro-Bond resin. Antibodies were eluted from the resin by exposure to transient low pH which did not strip GldJ-His. For this purpose 50 μl of settled resin was exposed to 150 μl of 150 mM NaCl–100 mM sodium phosphate (pH 4.5), and 20 μl of 4 N HCl was added per 150 μl. The resin was pelleted by centrifugation, and the supernatant containing antibody was added to 50 μl of 500 mM Tris, pH 7.5.

Cell fractionation and Western blot analyses. *F. johnsoniae* cells were disrupted with a French press and fractionated into soluble and membrane fractions by centrifugation at 223,160 × *g* for 60 min as described previously (19). Proteins were separated by sodium dodecyl sulfate-polyacrylamide gel electrophoresis (SDS-PAGE), and Western blot analyses were performed as previously described (21).

In vivo radiolabeling with [^{3}H]palmitate and [^{3}H]glutamate. To identify lipoproteins, cells of *F. johnsoniae* were incubated for 3 h in SDY broth (0.5 mM $MgSO_4$, 0.05 mM $FeSO_4$, 0.04 mM EDTA, 0.2 mM $CaCl_2$, 18.7 mM NH_4Cl, 22.2 mM glucose, 0.1 g of yeast extract/liter, and 20 mM potassium phosphate, pH 7.25) containing 50 μCi of either [9,10-^{3}H]palmitate (48 Ci/mmol) or L-[3,4-^{3}H]glutamic acid (51 Ci/mmol; Perkin-Elmer Life Sciences, Boston, Mass.)/ml, and radiolabeled proteins were separated by SDS-PAGE and detected by autoradiography as previously described (31). To determine whether GldJ is a lipoprotein, cells expressing GldJ-His were labeled with [^{3}H]palmitate and [^{3}H]glutamate as previously described (31). Cells were lysed, recombinant His-tagged proteins were isolated using Ni-NTA His-Bind resin (Novagen, Madison, Wis.) and separated by SDS-PAGE, and radiolabeled proteins were detected by autoradiography as described previously (31).

Microscopic observations. Wild-type and mutant cells of *F. johnsoniae* were examined for movement over glass and agar surfaces and for their ability to propel polystyrene latex spheres by phase-contrast microscopy as previously described (31).

Cells of wild-type *F. johnsoniae* UW101 and of the *gldJ* mutant UW102-48 were analyzed by immunofluorescence confocal microscopy to localize GldJ. Cultures were grown to early stationary phase in CYE broth at 25°C, and motility was assayed by light microscopy prior to sample preparation to ensure that most cells were actively motile. Cells were pelleted by centrifugation, suspended in 10 mM Tris (pH 7.5), and spotted onto microscope slides that had been coated with poly-L-lysine. Slides were incubated for 5 min at 25°C to allow cells to settle, formaldehyde was added to a 1% final concentration, and the cells were fixed for 15 min at 25°C. Cells were permeabilized by two 30-min incubations at 22°C in 100 μl of 25 mM Tris (pH 7.5)–5 mM EDTA–2% Triton X-100. Permeabilized cells were washed three times by gently dipping the slide into 50 ml of 25 mM sodium phosphate (pH 7.5)–100 mM NaCl (phosphate-buffered saline [PBS]) and were blocked with 100 μl of PBS containing 1% bovine serum albumin for 30 min at 22°C. Cells were exposed to affinity-purified anti-GldJ polyclonal antiserum (1:200 dilution) in PBS plus 1% bovine serum albumin at 4°C for 16 h. Samples were washed three times in PBS and incubated with anti-rabbit secondary antibody conjugated with an Alexa 488 chromophore (Molecular Probes) in PBS plus 1% bovine serum albumin for 2 h at 22°C. Cells were washed three times with PBS, antifade was added, and a coverslip was sealed over the cells with nail polish. Samples were observed using a Leica TCS SP2 confocal system.

Sample preparation for transmission electron microscopy was essentially the same as for confocal microscopy with the following modifications. Cells were settled onto Formvar- and polylysine-coated 400-mesh Ni grids before fixation. Washes were 1.5-ml volumes, and antibody incubations were 20-μl volumes as droplets on Parafilm. The secondary antibody was a dual-conjugated anti-rabbit Fab′ with an Alexa 488 chromophore and a 1.4-nm gold particle (Fluoronanogold; Nanoprobes Inc.). Gold particles were enlarged by silver enhancement for 4 min at 22°C in the dark with the Silver HQ kit (Nanoprobes Inc.), and samples were examined using a Hitachi H-600 transmission electron microscope at 75 kV.

Measurements of bacteriophage sensitivity. Sensitivity to *F. johnsoniae* bacteriophages was determined essentially as previously described by spotting 5 μl of phage lysates (6×10^7 PFU/ml) onto lawns of cells in CYE overlay agar (21). The plates were incubated for 24 h at 25°C to observe lysis.

Nucleotide sequence accession number. The sequence reported in this paper has been deposited in the GenBank database (accession no. AF527793).

RESULTS

Identification of *gldJ*. UW102-48 is a spontaneous nonmotile mutant of *F. johnsoniae* UW101 (7). Cells of UW102-48 formed nonspreading colonies on PY2 agar whereas wild-type cells formed spreading colonies (Fig. 2C and A). Wild-type cells also exhibited rapid motility in wet mounts and actively propelled latex spheres along their surfaces whereas cells of UW102-48 did not move in wet mounts and failed to propel spheres. A cosmid library containing wild-type *F. johnsoniae* DNA in pCP26 was transferred into UW102-48, and spreading colonies were obtained. pCP432 was isolated from one complemented colony. Introduction of pCP432 into UW102-48 restored the ability of cells to glide over glass surfaces, to propel latex spheres, and to form spreading colonies. Subclones of pCP432 were used to determine the minimal region required for complementation. Introduction of pMM265, pMM313, and pMM314 (each of which spans *gldJ*) into UW102-48 resulted in complementation (Fig. 2D and 1). The colonies spread over agar, and cells exhibited rapid gliding motility in wet mounts and propelled latex spheres. Colonies of UW102-48 complemented with pMM313 did not spread as well as wild-type cells but did spread as well as wild-type cells carrying pMM313 (Fig. 2, compare panels A, B, and D). Apparently introduction of *gldJ* into wild-type cells on pMM313, which has a copy number of approximately 10, resulted in partial inhibition of colony spreading. Introduction of pMM317 and pMM318 (which encode the first 337 and 547 amino acids of GldJ, respectively) resulted in a more dramatic inhibition of colony spreading. These plasmids failed to restore motility to UW102-48, and introduction of either plasmid into

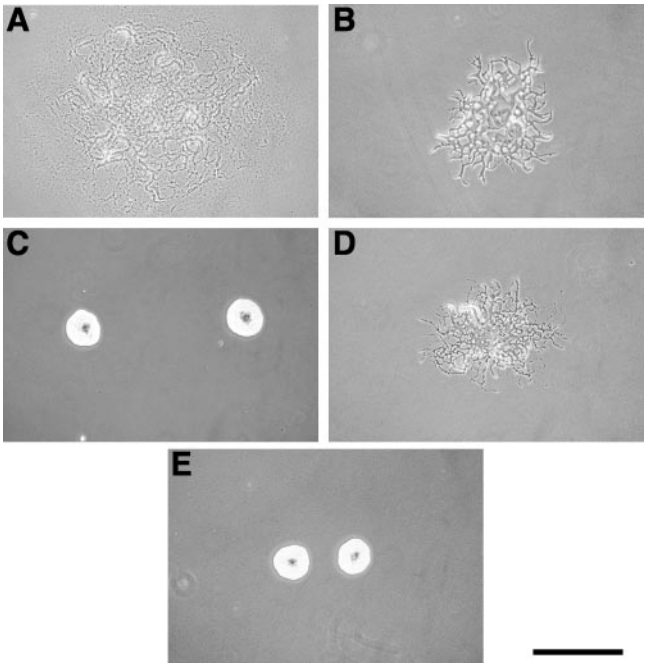

FIG. 2. Photomicrographs of *F. johnsoniae* colonies. Colonies were grown for 30 h at 25°C on PY2 agar medium containing 100 μg of erythromycin/ml. Photomicrographs were taken with a Kodak DC290 digital camera mounted on an Olympus IMT-2 inverted microscope. Bar, 1 mm. (A) Wild-type *F. johnsoniae* UW101 with shuttle vector pCP11. (B) Wild-type cells with pMM313, which carries *gldJ*. (C) *gldJ* mutant UW102-48 with pCP11. (D) UW102-48 complemented with pMM313. (E) Wild-type cells with pMM317, which carries a truncated version of *gldJ*.

wild-type cells resulted in severe motility defects (Fig. 2E and data not shown). Colonies of wild-type cells carrying pMM317 formed nonspreading colonies, and most cells failed to move in wet mounts. Wild-type cells carrying pMM318 exhibited greater motility than those carrying pMM317 but were far less motile than cells without *gldJ* on a plasmid. Apparently the truncated proteins prevented the wild-type protein from functioning properly.

Analysis of *gldJ* and surrounding DNA. The *gldJ* coding region is 1,683 nucleotides in length and encodes a predicted protein of 561 amino acids. A sequence which matches the *Bacteroides* consensus promoter region (TAXXTTTG) (3) ends 123 bp upstream of the *gldJ* start codon, and a 17-bp inverted repeat which may function as a transcription terminator starts 18 bp downstream of the *gldJ* stop codon. Analysis of the amino acid sequence suggests that GldJ has a cleavable signal peptide. The predicted molecular mass of GldJ (after cleavage of its signal peptide) is 63.6 kDa. GldJ exhibits sequence similarity to a protein of unknown function from the distantly related gliding bacterium *Cytophaga hutchinsonii* (GenBank accession no. ZP00308187). The *C. hutchinsonii* protein is 165 amino acids shorter than *F. johnsoniae* GldJ but exhibits 44.7% amino acid identity with GldJ over its entire sequence if several large gaps are allowed. *F. johnsoniae* GldJ also exhibits more limited similarity to proteins that contain a domain of unknown function known as DUF323. Proteins that carry this domain and are similar to GldJ include *Pectobacterium carotovorum* CarF (33% amino acid identity with GldJ over 121 amino acids), *Geobacillus stearothermophilus* XaiF (36% identity over 104 amino acids), and human SUMF1 (33% identity over 99 amino acids). CarF is involved in resistance to the β-lactam antibiotic carbapenem (33); XaiF is involved in the production, export, or activation of extracellular xylanase (8); and SUMF1 is an enzyme that activates sulfatases by converting a cysteine residue into the active-site formylglycine (9, 11). Given the diverse functions of these proteins and their limited regions of similarity with GldJ, the exact function of GldJ remains uncertain.

fjo23 and *fjo24*, which lie upstream of and are transcribed divergently from *gldJ*, do not exhibit significant similarity to genes of known function (Fig. 1). *murF* lies downstream of *gldJ* and encodes a protein that is 33% identical over 441 amino acids to MurF of *Bacillus licheniformis*, which is involved in peptidoglycan synthesis (40). *fjo25* and *fjo26*, which lie downstream of *murF*, encode proteins that are similar to putative two-component signal transduction proteins and to the outer membrane protein SusC of *Bacteroides thetaiotaomicron*, respectively (39). There is no evidence linking *murF*, *fjo23*, *fjo24*, *fjo25*, or *fjo26* with gliding motility.

Identification of additional *gldJ* mutants. UW102-48 is one of 50 spontaneous and chemically induced nonmotile mutants isolated by Pate and colleagues (7, 51). Introduction of pCP432 restored motility to 11 mutants in addition to UW102-48. pMM265, which spans just *gldJ*, restored motility to each of the 12 mutants that were complemented by pCP432 but did not complement any of the other 38 mutants. The exact site of mutation in each *gldJ* mutant was determined by amplification and sequencing. Seven of the mutants carried frameshift mutations (UW102-21, T deleted at position 772 numbered from the A of the *gldJ* start codon; UW102-48, A deleted at position 588; UW102-55, G inserted after position 88; UW102-80, A deleted at position 598; UW102-86, A deleted at position 452 and C-to-T transition at position 453; UW102-96, T deleted at position 501; and UW102-348, A inserted after position 81). The remaining five mutants had base substitutions (UW102-66, G to C at position 534; UW102-81, A to T at position 1627; UW102-95, T to G at position 1088; UW102-100, T to G at position 312; UW102-301, T to G at position 1088).

GldJ is a lipoprotein. The predicted amino-terminal sequence of GldJ (MKVNKIVVLQLMMSMVLMLGTASC SKK) contains a hydrophobic stretch terminated by a cysteine (underlined), which is characteristic of lipoproteins (17). Lipoproteins undergo a series of modifications that result in cleavage of the signal peptide and covalent attachment of fatty acids to the amino-terminal cysteine (17). To determine whether GldJ was a lipoprotein, *F. johnsoniae* cells were labeled with [^{3}H]palmitate as described in Materials and Methods. In a parallel experiment cells were incubated with [^{3}H]glutamate to label essentially all proteins (Fig. 3A, lane 1). A limited subset of wild-type cell proteins were labeled with [^{3}H]palmitate (Fig. 3A, lane 2) confirming that, as previously described, label from [^{3}H]palmitate was not rapidly incorporated into amino acids (31). Cells of the *gldJ* mutant UW102-48 exhibited a lipoprotein profile that was similar to that of wild-type cells, except that a band of approximately 70 kDa, which is close to the expected size of GldJ, was absent (Fig. 3A, lane 11). Complementation of UW102-48 with pMM265, which has

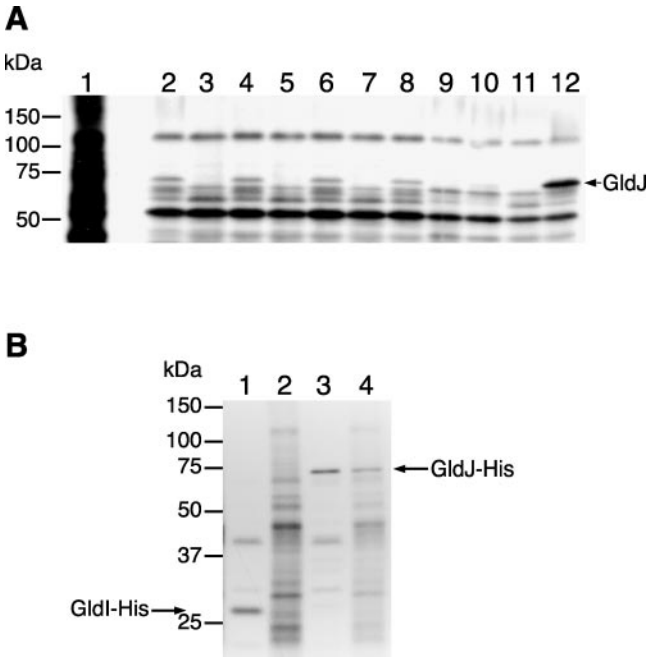

FIG. 3. GldJ is a lipoprotein. (A) Cells of *F. johnsoniae* were labeled with either [^{3}H]glutamate (to label nearly all proteins) or [^{3}H]palmitate (to label lipoproteins). Proteins were separated by SDS-PAGE and detected by autoradiography. Lane 1 contains extracts of wild-type cells labeled with [^{3}H]glutamate, whereas the remaining lanes contain extracts of wild-type, mutant, or complemented cells labeled with [^{3}H]palmitate. Lane 2, wild-type *F. johnsoniae*. Lane 3, *gldB* mutant CJ569. Lane 4, CJ569 complemented with pDH233, which carries wild-type *gldB*. Lane 5, *gldD* mutant CJ282. Lane 6, CJ282 complemented with pMM213, which carries wild-type *gldD*. Lane 7, *gldH* mutant CJ1043. Lane 8, CJ1043 complemented with pMM293, which carries wild-type *gldH*. Lane 9, *gldI* mutant UW102-41. Lane 10, UW102-41 complemented with pMM291, which carries wild-type *gldI*. Lane 11, *gldJ* mutant UW102-48. Lane 12, UW102-48 complemented with pMM265, which carries wild-type *gldJ*. (B) Radiolabeling of GldI-His and GldJ-His. Cells of *F. johnsoniae* were labeled with [^{3}H]palmitate or [^{3}H]glutamate. Proteins were isolated by precipitation with Ni-NTA His-Bind resin, separated by SDS-PAGE, and detected by autoradiography. Lane 1, cells expressing GldI-His from pTB45, labeled with [^{3}H]palmitate. Lane 2, cells expressing GldI-His from pTB45, labeled with [^{3}H]glutamate. Lane 3, cells expressing GldJ-His from pTB44, labeled with [^{3}H]palmitate. Lane 4, cells expressing GldJ-His from pTB44, labeled with [^{3}H]glutamate.

a copy number of approximately 10 in *F. johnsoniae*, resulted in overexpression of GldJ lipoprotein (Fig. 3A, lane 12). To verify that the 70-kDa protein was GldJ, pTB44, which expresses recombinant GldJ carrying eight histidine residues at its carboxy terminus, was introduced into *F. johnsoniae* UW102-48. GldJ-His was functional since it restored motility to the mutant. Cells were incubated with [^{3}H]palmitate or [^{3}H]glutamate, and proteins were isolated using Ni-NTA His-Bind resin. The eluted proteins were separated by SDS-PAGE, and radiolabeled proteins were detected by autoradiography. Cells expressing the lipoprotein GldI-His from pTB45 (30) were processed similarly as a positive control. GldJ-His, which migrated with an apparent molecular mass of approximately 70 kDa, was labeled by [^{3}H]palmitate, suggesting that it is a lipoprotein (Fig. 3B, lane 3). Incubation with [^{3}H]palmitate resulted in more intense labeling of GldJ-His than did incubation with

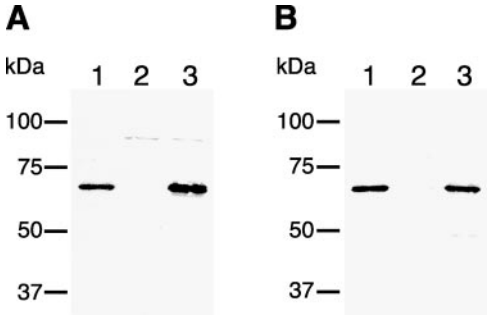

FIG. 4. Immunodetection of GldJ. (A) Whole-cell extracts were examined for GldJ by Western blot analysis. Lane 1, wild-type *F. johnsoniae*. Lane 2, *gldJ* mutant UW102-48. Lane 3, UW102-48 with pMM313, which carries *gldJ*. Equal amounts of protein were loaded in each lane. (B) Cell fractions of wild-type *F. johnsoniae* were examined for GldJ by Western blot analysis. Lane 1, whole cells. Lane 2, soluble fraction. Lane 3, membrane fraction. Equal amounts of protein were loaded in each lane.

[^{3}H]glutamate (Fig. 3B, lanes 3 and 4), suggesting that labeling was not the result of metabolism of [^{3}H]palmitate into amino acids before incorporation. Cells carrying pTB45 produced radiolabeled GldI-His but did not produce any labeled proteins of greater than 50 kDa (Fig. 3B, lane 1), confirming that the 70-kDa band in Fig. 3B, lane 3, was GldJ-His. Cells with mutations in *gldB*, *gldD*, *gldH*, and *gldI* failed to produce radiolabeled GldJ (Fig. 3A, lanes 3, 5, 7, and 9). Complementation with wild-type *gldB*, *gldD*, *gldH*, and *gldI*, respectively, restored the ability to form labeled GldJ lipoprotein (Fig. 3A, lanes 4, 6, 8, and 10).

Immunodetection of GldJ. Antisera to GldJ were used to detect GldJ in cell extracts. GldJ, which migrated with an apparent molecular mass of approximately 70 kDa, was detected in extracts of wild-type cells (Fig. 4A, lane 1) but was absent from extracts of the *gldJ* mutant UW102-48 (Fig. 4A, lane 2). Introduction of *gldJ* on pMM313 restored production of GldJ (Fig. 4A, lane 3). As expected of a lipoprotein, GldJ was found primarily in the membrane fraction of wild-type cells (Fig. 4B).

As mentioned above, mutations in *gldB*, *gldD*, *gldH*, and *gldI* resulted in decreased levels of labeled GldJ lipoprotein. This could be a result of decreased GldJ protein or decreased lipid modification of GldJ. Western blot analyses were used to determine whether mutations in *gld* genes resulted in decreased levels of GldJ protein. Disruption of *gldA*, *gldB*, *gldD*, *gldF*, *gldG*, *gldH*, or *gldI* resulted in normal levels of *gldJ* transcript (Fig. 5A) but a dramatic reduction in GldJ protein (Fig. 5B). This may indicate that GldJ interacts directly or indirectly with the products of these genes and that removal of any one of these proteins destabilizes GldJ. Introduction of pMM317 and pMM318, which encode truncated forms of GldJ, into wild-type cells resulted in motility defects as mentioned above and also resulted in reduction of GldJ levels (data not shown). Truncated GldJ protein was also barely detectable in these cells. In contrast to the effect of mutations in *gldA* to *gldI* on GldJ levels, mutations in *gldJ* did not alter the levels of GldA, GldB, GldD, or GldH as determined by comparison of Western blots of wild-type cells and of cells of the *gldJ* mutant UW102-80 (data not shown).

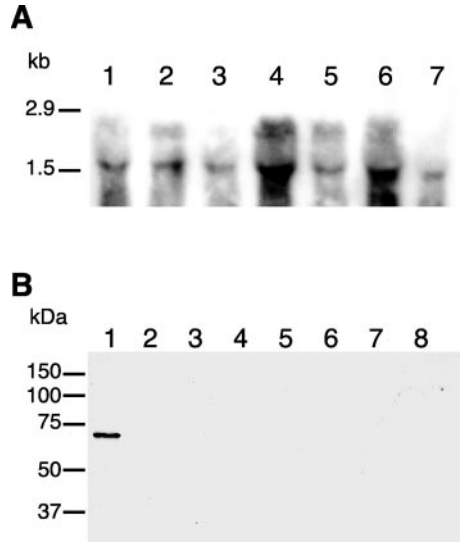

FIG. 5. Effect of *gld* mutations on levels of *gldJ* mRNA and GldJ protein. (A) Northern blot analysis. RNA was isolated from wild-type and mutant cells and probed with digoxigenin-labeled *gldJ* RNA. Lane 1, wild-type *F. johnsoniae* UW101. Lane 2, *gldA* mutant CJ101-288. Lane 3, *gldB* mutant CJ569. Lane 4, *gldD* mutant CJ282. Lane 5, *gldFG* mutant CJ787. Lane 6, *gldH* mutant CJ1043. Lane 7, *gldI* mutant UW102-41. Equal amounts of RNA were loaded in each lane. (B) Western blot analysis of whole-cell extracts with the use of antiserum to GldJ. Lane 1, wild-type *F. johnsoniae* UW101. Lane 2, *gldJ* mutant UW102-80, Lane 3, *gldA* mutant CJ101-288. Lane 4, *gldB* mutant CJ569. Lane 5, *gldD* mutant CJ282. Lane 6, *gldFG* mutant CJ787. Lane 7, *gldH* mutant CJ1043. Lane 8, *gldI* mutant UW102-41. Equal amounts of protein were loaded in each lane.

Localization of GldJ by immunofluorescence microscopy and transmission electron microscopy. The availability of a specific antiserum to GldJ allowed us to determine the localization of GldJ in cells of *F. johnsoniae*. Addition of antiserum to cells did not disrupt gliding, and intact cells did not absorb significant amounts of anti-GldJ antibodies as detected by immunofluorescence microscopy, suggesting that most of the GldJ was not exposed on the cell surface. Analysis of fixed, permeabilized cells allowed detection of GldJ by immunofluorescence microscopy and by immunoelectron microscopy (Fig. 6). In both cases GldJ was organized in discrete bands that appeared to form a helical structure in a significant fraction of cells observed, suggesting that at least part of the machinery involved in cell movement is arranged in a helical array in the cell envelope. The structures observed on different cells did not conform to a single helical pitch. Of 111 cells examined by immunoelectron microscopy, 69 displayed labeling of apparent helical structures, 12 exhibited monopolar localization of GldJ (some of these also exhibited partial helical labeling), 4 were undergoing cell division and exhibited midcell division plane localization, and the remaining 26 displayed labeling that was not obviously associated with any regular structure. The midcell localization of GldJ in dividing cells was examined further by identifying additional dividing cells. Each of 25 cells observed to have cell division cross walls exhibited intense labeling near the division plane (Fig. 6B and C and data not shown).

***gldJ* mutants are resistant to bacteriophage infection.** Many nonmotile mutants of *F. johnsoniae* are resistant to infection by a number of *F. johnsoniae* bacteriophages (50). The reason for this pleiotropy is not known. The sensitivity of wild-type and *gldJ* mutant cells to bacteriophages was tested. Wild-type cells of *F. johnsoniae* were readily lysed (Fig. 7A), whereas 11 of the 12 *gldJ* mutants were resistant to infection by each of the bacteriophages (Fig. 7B and data not shown). The exception was UW102-48, which was slightly sensitive to three of eight phages tested (ϕCj42, ϕCj48, and ϕCj54), resulting in the formation of turbid zones of partial lysis (Fig. 7D). Introduction of wild-type *gldJ* on pMM313 into the *gldJ* mutants UW102-48, UW102-55, UW102-66, UW102-80, UW102-81, UW102-86, UW102-95, UW102-96, UW102-100, and UW102-301 restored sensitivity to each of the phages in addition to restoring gliding motility (Fig. 7C and E and data not shown). In contrast, introduction of pMM313 into the *gldJ* mutants UW102-21 and UW102-348 restored sensitivity to only some of the phages. Cells of UW102-21 carrying pMM313 were sensitive to six of the phages but remained resistant to ϕ28 and ϕ29. UW102-21 carrying pMM313 exhibits weak motility, which may account for the resistance to some phages. Cells of UW102-348 carrying pMM313 were resistant to ϕ28, ϕ29, ϕ42, ϕ48, and ϕ54 and were only slightly sensitive to ϕ1, ϕ13, and ϕ23. This was surprising, since cells of UW102-348 carrying pMM313 exhibited good motility. UW102-348 may have mutations other than the defect in *gldJ* which result in phage resistance.

***gldJ* mutants are defective in chitin utilization.** Wild-type cells of *F. johnsoniae* rapidly digest chitin (47), whereas many nonmotile mutants are deficient in digestion of this insoluble polysaccharide (7, 30, 31). The effect of mutations in *gldJ* on chitin utilization was determined in MYA medium supplemented with chitin as the primary carbon, energy, and nitrogen source. Cells of each of the *gldJ* mutants were defective in chitin digestion (Fig. 8 and data not shown). Complementation with pMM313 restored the ability to digest chitin in addition to restoring gliding motility. Similar results were obtained when chitin utilization was tested on PY2-chitin medium, except that some limited degradation of chitin was observed for each of the *gldJ* mutants upon extended incubation. PY2-chitin medium contains peptone and yeast extract and allows growth of strains regardless of whether they are able to efficiently utilize chitin. Wild-type cells produced obvious clearing zones on PY2 chitin medium after 1 day of incubation, whereas the *gldJ* mutants produced similar zones of clearing only after 7 to 10 days of incubation. The limited chitin digestion displayed by the *gldJ* mutants did not appear to be the result of reversion. Cells from the zones of chitin digestion were streaked on PY2 agar, resulting in nonspreading growth with no spreading colonies or flares.

DISCUSSION

The mechanism of *F. johnsoniae* gliding motility is not known. Eight genes (*gldA*, *gldB*, *gldD*, *gldF*, *gldG*, *gldH*, *gldI*, and *ftsX*) that are required for gliding have previously been described (1, 19-21, 24, 30, 31). GldA, GldF, and GldG are thought to form an ABC transporter, but the functions of the other *gld* proteins are not known. *ftsX* is required for cell

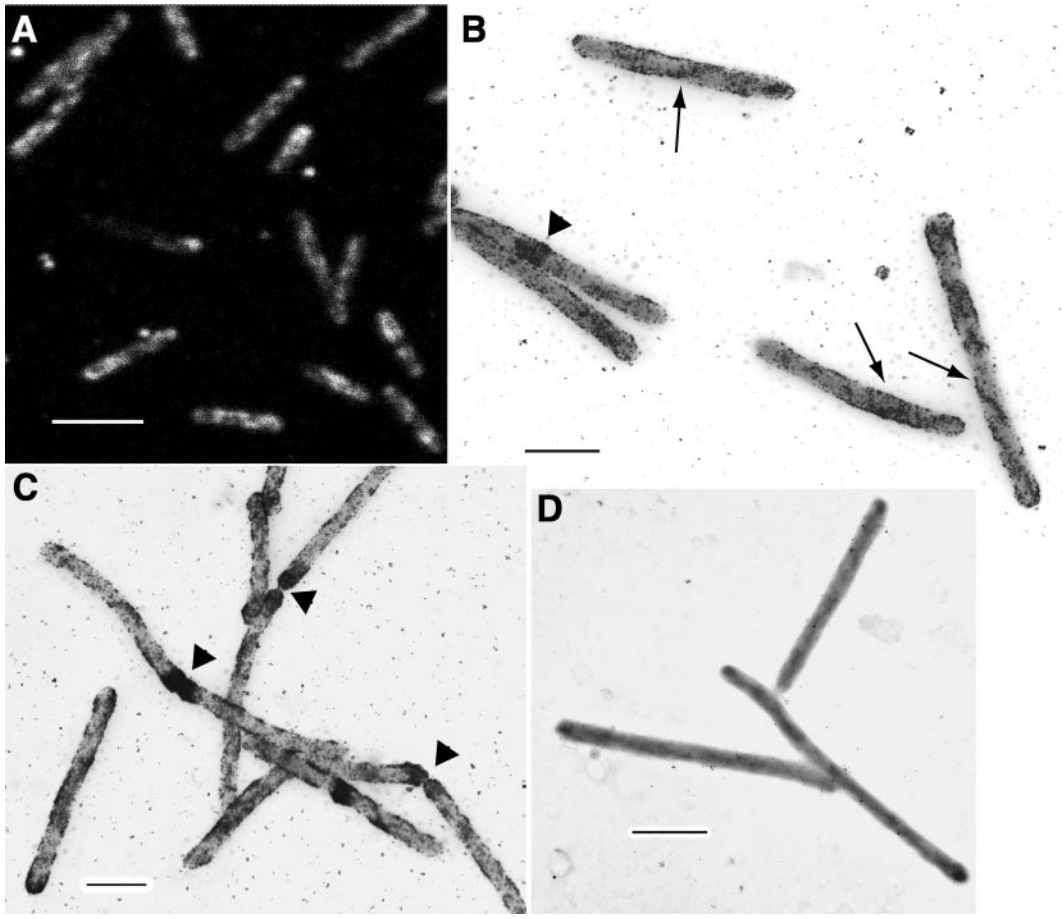

FIG. 6. Localization of GldJ by immunofluorescence microscopy and transmission electron microscopy. Cells of *F. johnsoniae* were fixed with 1% formaldehyde for 15 min and permeabilized with 5 mM EDTA and 2% Triton X-100, and GldJ was detected using affinity-purified antiserum. Cells were observed by confocal fluorescence microscopy (A) or by transmission electron microscopy (B to D). (A) Immunofluorescent image of wild-type cells incubated with antiserum to GldJ. (B) Electron microscopic image of wild-type cells incubated with antiserum to GldJ. (C) Wild-type cells undergoing cell division incubated with antiserum to GldJ. (D) Cells of the *gldJ* mutant UW102-48 incubated with antiserum to GldJ. Arrows in panel B indicate cells exhibiting labeling of helical structures. Large arrowheads in panels B and C indicate cells undergoing cell division. Bars, 4 (A) and 1 (B to D) μm.

division and for gliding motility. The results presented in this paper identify another gene, *gldJ*, that is required for gliding. *gldJ* encodes a 70-kDa lipoprotein. At least four other lipoproteins (GldB, GldD, GldH, and GldI) are also required for gliding (30, 31). We do not know why so many of the known Gld proteins are lipoproteins. The Gld proteins may assemble to form a multiprotein complex in the cell envelope, and membrane anchoring of the lipoproteins may be required for this. Disruption of any of the known *gld* genes results in normal levels of *gldJ* transcript but decreased levels of GldJ protein. The simplest explanation for these results is that GldJ is unstable in the absence of any other Gld protein, which is consistent with the suggestion that the Gld proteins form a complex. Expression in wild-type cells of truncated GldJ proteins from pMM317 and pMM318 disrupted motility and resulted in decreased levels of GldJ protein, which may indicate that GldJ forms oligomers. Incorporation of truncated GldJ may result in improper assemblies that are nonfunctional and are targeted for degradation. Alternatively, truncated GldJ may sequester and titrate out another Gld protein that is required to stabilize GldJ.

The properties of *gldJ* mutants were similar to those of previously described *gld* mutants (1, 19-21, 30, 31). In addition to complete loss of cell movement and colony spreading, cells of *gldJ* mutants, like those of other *gld* mutants, failed to propel latex spheres, were resistant to a variety of bacteriophages that infect wild-type cells, and were deficient in chitin digestion. Unlike previously characterized *gld* mutants, one of the *gldJ* mutants (UW102-48) was slightly sensitive to three of the eight phages tested. Cells of UW102-48 may produce a small amount of truncated GldJ protein that results in weak susceptibility to these phages. UW102-48 was originally reported to be resistant to all of these phages (7). The conditions employed in our experiments are slightly different than those used by previous investigators, which may account for the observed differences. While nearly all of the nonmotile mutants that we have analyzed are resistant to all phages tested, the finding of a nonmotile mutant that retains some susceptibility to phage infec-

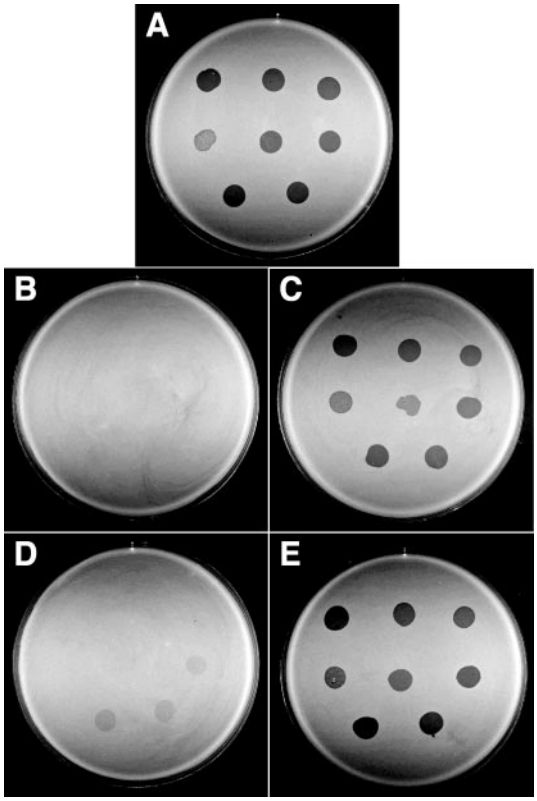

FIG. 7. Effect of mutations in *gldJ* on bacteriophage resistance. Bacteriophages (5 μl of lysates containing approximately 6×10^7 phage/ml) were spotted onto lawns of cells in CYE overlay agar containing 100 μg of erythromycin/ml. The plates were incubated at 25°C for 24 h to observe lysis. Bacteriophages were spotted in the following order from left to right: top row, ϕCj1, ϕCj13, and ϕCj23; middle row, ϕCj28, ϕCj29, and ϕCj42; bottom row, ϕCj48 and ϕCj54. (A) Wild-type *F. johnsoniae* with shuttle vector pCP11. (B) *gldJ* mutant UW102-55 with pCP11. (C) UW102-55 complemented with pMM313, which carries *gldJ*. (D) *gldJ* mutant UW102-48 with pCP11. (E) UW102-48 complemented with pMM313, which carries *gldJ*. The diameter of the petri dish is 9 cm.

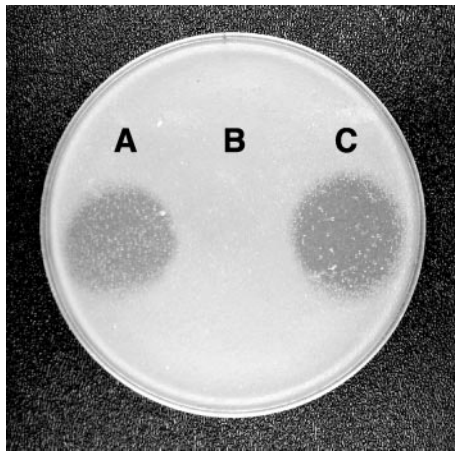

FIG. 8. Effect of mutation in *gldJ* on ability to utilize chitin. Approximately 4×10^7 cells of wild-type *F. johnsoniae* with shuttle vector pCP11 (A), of the *gldJ* mutant UW102-48 with pCP11 (B), and of UW102-48 complemented with pMM313, which carries *gldJ* (C), were spotted on MYA-chitin medium containing 100 μg of erythromycin/ml and incubated for 4 days at 25°C.

tion is not entirely novel, since others have reported that some nonmotile mutants are sensitive to some phages (16). The connection among bacteriophage resistance, chitin utilization, and gliding motility is not understood. It has previously been suggested that gliding, bacteriophage sensitivity, and chitin utilization may each rely on one or more transporters that are defective in *gld* mutants (31).

The known *gld* genes comprise many, but not all, of the genes required for gliding. Pate and colleagues isolated 50 spontaneous or chemically induced nonmotile mutants of *F. johnsoniae* (7, 21, 51). Introduction of *gldA*, *gldB*, *gldD*, *gldF*, *gldG*, *gldH*, *gldI*, and *gldJ* individually into these mutants restored motility to 33 of them (references 1, 19-21, 30, and 31 and this study). Apparently, these eight genes constitute a significant fraction of the genes required for gliding.

Immunofluorescence microscopy and immunoelectron microscopy identified bands of GldJ that appeared to be arranged in a helical manner. Recently it has become clear that many proteins involved in cell division, chromosome partitioning, and other processes are arranged helically within the cytoplasm, cytoplasmic membrane, or outer membrane of bacterial cells (6, 12-14, 22, 45). Newly synthesized peptidoglycan may also have a helical arrangement (10, 34). The relationship of any of these helical structures to GldJ is not known, but they could provide a scaffold on which GldJ is mounted. Helical structures in *F. johnsoniae* cells were previously observed by scanning electron microscopy (26), but their relationship to motility was uncertain since mutants were not analyzed. Observations of rotation of the cell body during movement have also been reported for some gliding bacteria related to *F. johnsoniae* (4, 15, 41) and are consistent with a helical arrangement of some components of the motility apparatus.

The observation that GldJ was localized near the division plane of dividing cells may have implications regarding the mechanism of gliding. A previous study demonstrated that mutations in *ftsX* resulted in defects in both cell division and gliding motility and that wild-type cells appeared to stop gliding during cell division (24). The localization of GldJ near the division plane adds another link between gliding motility and cell division. The gliding motility machinery and the cell division apparatus may share some components. For example, gliding could rely on components of the cytoskeleton that are also involved in cell division. Alternatively, the wall restructuring that occurs during cell division may be incompatible with functioning of the motility apparatus, resulting in temporary cessation of movement and accumulation of *gldJ* near the septum.

GldJ is required for gliding motility and for efficient chitin utilization, but its exact functions in these processes are not known. The apparently helical arrays of GldJ may be the first glimpse of the *F. johnsoniae* motility machinery. The available data suggest two possible models to describe gliding motility. The requirement of a transporter for gliding and the correlation between loss of motility and loss of ability to utilize chitin support the idea that motility is powered by coordinated export and import of macromolecules across the outer membrane, forming a "conveyor belt" along the cell surface (29, 31).

Chitin utilization may involve transport of long chitin oligomers across the outer membrane with the use of some of the machinery that is required for gliding (30, 31). The helical arrangement of GldJ suggests alternative models that rely on movements of the helical structures within the periplasm or movements of outer membrane components along a helical framework. These movements could require the activities of cytoplasmic membrane proteins and cytoskeletal proteins. Given the novelty of the proteins required for gliding, other mechanisms are also possible. Further analysis of GldJ and of other proteins required for cell movement will help determine the actual mechanism of *F. johnsoniae* gliding motility.

ACKNOWLEDGMENTS

This research was supported by a grant from the National Science Foundation (MCB-0130967) and by a Milwaukee Foundation Shaw Scientist Award to M.J.M.

We thank H. Owen for assistance with confocal microscopy and electron microscopy, J. Wahlberg for construction of pJW201, and D. Saffarini for careful reading of the manuscript.

REFERENCES

1. **Agarwal, S., D. W. Hunnicutt, and M. J. McBride.** 1997. Cloning and characterization of the *Flavobacterium johnsoniae* (*Cytophaga johnsonae*) gliding motility gene, *gldA*. Proc. Natl. Acad. Sci. USA **94:**12139–12144.
2. **Altschul, S. F., W. Gish, W. Miller, E. W. Myers, and D. J. Lipman.** 1990. Basic local alignment search tool. J. Mol. Biol. **215:**403–410.
3. **Bayley, D. P., E. R. Rocha, and C. J. Smith.** 2000. Analysis of *cepA* and other *Bacteroides fragilis* genes reveals a unique promoter structure. FEMS Microbiol. Lett. **193:**149–154.
4. **Beatson, P. J., and K. C. Marshall.** 1994. A proposed helical mechanism for gliding motility in three gliding bacteria (order *Cytophagales*). Can. J. Microbiol. **40:**173–183.
5. **Bhaya, D., N. R. Bianco, D. Bryant, and A. R. Grossman.** 2000. Type IV pilus biogenesis and motility in the cyanobacterium *Synechocystis* sp. PCC6803. Mol. Microbiol. **37:**941–951.
6. **Campo, N., H. Tjalsma, G. Buist, D. Stepniak, M. Meijer, M. Veenhuis, M. Westermann, J. Muller, S. Bron, J. Kok, O. Kuipers, and J. Jongbloed.** 2004. Subcellular sites for bacterial protein export. Mol. Microbiol. **53:**1583–1599.
7. **Chang, L. Y. E., J. L. Pate, and R. J. Betzig.** 1984. Isolation and characterization of nonspreading mutants of the gliding bacterium *Cytophaga johnsonae*. J. Bacteriol. **159:**26–35.
8. **Cho, S. G., and Y. J. Choi.** 1998. Characterization of the *xaiF* gene encoding a novel xylanase-activity-increasing factor, XaiF. J. Microbiol. Biotechnol. **8:**378–387.
9. **Cosma, M., S. Pepe, I. Annunziata, R. Newbold, M. Grompe, G. Parenti, and A. Ballabio.** 2003. The multiple sulfatase deficiency gene encodes an essential and limiting factor for the activity of sulfatases. Cell **113:**445–456.
10. **Daniel, R., and J. Errington.** 2003. Control of cell morphogenesis in bacteria: two distinct ways to make a rod-shaped cell. Cell **113:**767–776.
11. **Dierks, T., B. Schmidt, L. Borissenko, J. Peng, A. Preusser, M. Mariappan, and K. von Figura.** 2003. Multiple sulfatase deficiency is caused by mutations in the gene encoding the human C(alpha)-formylglycine generating enzyme. Cell **113:**435–444.
12. **Ebersbach, G., and K. Gerdes.** 2004. Bacterial mitosis: partitioning protein ParA oscillates in spiral-shaped structures and positions plasmids at mid-cell. Mol. Microbiol. **52:**385–398.
13. **Figge, R., A. Divakaruni, and J. Gober.** 2004. MreB, the cell shape-determining bacterial actin homologue, co-ordinates cell wall morphogenesis in *Caulobacter crescentus*. Mol. Microbiol. **51:**1321–1332.
14. **Gibbs, K., D. Isaac, J. Xu, R. Hendrix, T. Silhavy, and J. Theriot.** 2004. Complex spatial distribution and dynamics of an abundant *Escherichia coli* outer membrane protein, LamB. Mol. Microbiol. **53:**1771–1783.
15. **Godwin, S. L., M. Fletcher, and R. P. Burchard.** 1989. Interference reflection microscopic study of association between gliding bacteria and glass substrata. J. Bacteriol. **171:**4589–4594.
16. **Gorski, L., W. Godchaux III, E. R. Leadbetter, and R. R. Wagner.** 1992. Diversity in surface features of *Cytophaga johnsonae* motility mutants. J. Gen. Microbiol. **138:**1767–1772.
17. **Hayashi, S., and H. C. Wu.** 1990. Lipoproteins in bacteria. J. Bioenerg. Biomembr. **22:**451–471.
18. **Hoiczyk, E., and W. Baumeister.** 1998. The junctional pore complex, a prokaryotic secretion organelle, is the molecular motor underlying gliding motility in cyanobacteria. Curr. Biol. **8:**1161–1168.
19. **Hunnicutt, D. W., M. J. Kempf, and M. J. McBride.** 2002. Mutations in *Flavobacterium johnsoniae gldF* and *gldG* disrupt gliding motility and interfere with membrane localization of GldA. J. Bacteriol. **184:**2370–2378.
20. **Hunnicutt, D. W., and M. J. McBride.** 2001. Cloning and characterization of the *Flavobacterium johnsoniae* gliding motility genes *gldD* and *gldE*. J. Bacteriol. **183:**4167–4175.
21. **Hunnicutt, D. W., and M. J. McBride.** 2000. Cloning and characterization of the *Flavobacterium johnsoniae* gliding motility genes, *gldB* and *gldC*. J. Bacteriol. **182:**911–918.
22. **Jones, L., R. Carballido-Lopez, and J. Errington.** 2001. Control of cell shape in bacteria: helical, actin-like filaments in *Bacillus subtilis*. Cell **104:**913–922.
23. **Kaiser, D.** 2000. Bacterial motility: how do pili pull? Curr. Biol. **10:**R777–R780.
24. **Kempf, M. J., and M. J. McBride.** 2000. Transposon insertions in the *Flavobacterium johnsoniae ftsX* gene disrupt gliding motility and cell division. J. Bacteriol. **182:**1671–1679.
25. **Korolev, E. V., A. V. Nikonov, M. S. Brudnaya, E. S. Snigirevskaya, G. V. Sabinin, Y. Y. Komissarchik, P. I. Ivanov, and S. N. Borchsenius.** 1994. Tubular structures of *Mycoplasma gallisepticum* and their possible participation in cell motility. Microbiology **140:**671–681.
26. **Lunsdorf, H., and H. U. Schairer.** 2001. Frozen motion of gliding bacteria outlines inherent features of the motility apparatus. Microbiology **147:**939–947.
27. **Mattick, J.** 2002. Type IV pili and twitching motility. Annu. Rev. Microbiol. **56:**289–314.
28. **McBride, M. J.** 2001. Bacterial gliding motility: multiple mechanisms for cell movement over surfaces. Annu. Rev. Microbiol. **55:**49–75.
29. **McBride, M. J.** 2004. Cytophaga-flavobacterium gliding motility. J. Mol. Microbiol. Biotechnol. **7:**63–71.
30. **McBride, M. J., and T. F. Braun.** 2004. GldI is a lipoprotein that is required for *Flavobacterium johnsoniae* gliding motility and chitin utilization. J. Bacteriol. **186:**2295–2302.
31. **McBride, M. J., T. F. Braun, and J. L. Brust.** 2003. *Flavobacterium johnsoniae* GldH is a lipoprotein that is required for gliding motility and chitin utilization. J. Bacteriol. **185:**6648–6657.
32. **McBride, M. J., and M. J. Kempf.** 1996. Development of techniques for the genetic manipulation of the gliding bacterium *Cytophaga johnsonae*. J. Bacteriol **178:**583–590.
33. **McGowan, S. J., M. Sebaihia, S. O'Leary, K. R. Hardie, P. Williams, G. S. Stewart, B. W. Bycroft, and G. P. Salmond.** 1997. Analysis of the carbapenem gene cluster of *Erwinia carotovora*: definition of the antibiotic biosynthetic genes and evidence for a novel beta-lactam resistance mechanism. Mol. Microbiol. **26:**545–556.
34. **Mendelson, N.** 1976. Helical growth of *Bacillus subtilis*: a new model of cell growth. Proc. Natl. Acad. Sci. USA **73:**1740–1747.
35. **Miyata, M., H. Yamamoto, T. Shimizu, A. Uenoyama, C. Citti, and R. Rosengarten.** 2000. Gliding mutants of *Mycoplasma mobile*: relationships between motility and cell morphology, cell adhesion and microcolony formation. Microbiology **146:**1311–1320.
36. **Nakai, K., and M. Kanehisa.** 1991. Expert system for predicting protein localization sites in Gram-negative bacteria. Proteins Struct. Funct. Genet. **11:**95–110.
37. **Pate, J. L., S. J. Petzold, and L.-Y. E. Chang.** 1979. Phages for the gliding bacterium *Cytophaga johnsonae* that infect only motile cells. Curr. Microbiol. **2:**257–262.
38. **Pearson, W. R.** 1990. Rapid and sensitive sequence comparison with FASTP and FASTA. Methods Enzymol. **183:**63–98.
39. **Reeves, A. R., J. N. D'Elia, J. Frias, and A. A. Salyers.** 1996. A *Bacteroides thetaiotamicron* outer membrane protein that is essential for utilization of maltooligosaccharides and starch. J. Bacteriol. **178:**823–830.
40. **Rey, M., P. Ramaiya, B. Nelson, S. Brody-Karpin, E. Zaretsky, M. Tang, A. Lopez de Leon, H. Xiang, V. Gusti, I. Clausen, P. Olsen, M. Rasmussen, J. Andersen, P. Jorgensen, T. Larsen, A. Sorokin, A. Bolotin, A. Lapidus, N. Galleron, S. Ehrlich, and R. Berka.** 2004. Complete genome sequence of the industrial bacterium *Bacillus licheniformis* and comparisons with closely related *Bacillus* species. Genome Biol. **5:**R77.
41. **Ridgway, H. F., and R. A. Lewin.** 1988. Characterization of gliding motility in *Flexibacter polymorphus*. Cell Motil. Cytoskelet. **11:**46–63.
42. **Sambrook, J., E. F. Fritsch, and T. Maniatis.** 1989. Molecular cloning: a laboratory manual. Cold Spring Harbor Laboratory, Cold Spring Harbor, N.Y.
43. **Sawers, G., and A. Bock.** 1989. Novel transcriptional control of the pyruvate formate-lyase gene: upstream regulatory sequences and multiple promoters regulate anaerobic expression. J. Bacteriol. **171:**2485–2498.
44. **Schenk, P., S. Baumann, R. Mattes, and H. Steinbiss.** 1995. Improved high-level expression system for eukaryotic genes in *Escherichia coli* using T7 RNA polymerase and rare Arg tRNAs. BioTechniques **19:**196–200.
45. **Shih, Y., T. Le, and, R. L.** 2003. Division site selection in *Escherichia coli* involves dynamic redistribution of Min proteins within coiled structures that extend between the two cell poles. Proc. Natl. Acad. Sci. USA **100:**7865–7870.
46. **Simon, R., U. Priefer, and A. Puhler.** 1983. A broad host range mobilization

system for in vivo genetic engineering: transposon mutagenesis in Gram negative bacteria. Bio/Technology **2:**784–791.

47. **Stanier, R. Y.** 1947. Studies on nonfruiting myxobacteria. I. Cytophaga johnsonae, n. sp., a chitin-decomposing myxobacterium. J. Bacteriol. **53:**297–315.
48. **Sun, H., D. R. Zusman, and W. Shi.** 2000. Type IV pilus of *Myxococcus xanthus* is a motility apparatus controlled by the *frz* chemosensory system. Curr. Biol. **10:**1143–1146.
49. **Wolgemuth, C., E. Hoiczyk, D. Kaiser, and G. Oster.** 2002. How myxobacteria glide. Curr. Biol. **12:**369–377.
50. **Wolkin, R. H., and J. L. Pate.** 1986. Phage adsorption and cell adherence are motility-dependent characteristics of the gliding bacterium *Cytophaga johnsonae*. J. Gen. Microbiol. **132:**355–367.
51. **Wolkin, R. H., and J. L. Pate.** 1985. Selection for nonadherent or nonhydrophobic mutants co-selects for nonspreading mutants of *Cytophaga johnsonae* and other gliding bacteria. J. Gen. Microbiol. **131:**737–750.